

Eccentricity generation in hierarchical triple systems with non-coplanar and initially circular orbits

Nikolaos Georgakarakos (ng@maths.ed.ac.uk)

School of Mathematics, Edinburgh University, Mayfield Road, Edinburgh EH9 3JZ, UK

Abstract. In a previous paper, we developed a technique for estimating the inner eccentricity in coplanar hierarchical triple systems on initially circular orbits, with comparable masses and with well separated components, based on an expansion of the rate of change of the Runge-Lenz vector. Now, the same technique is extended to non-coplanar orbits. However, it can only be applied to systems with $I_0 < 39.23^\circ$ or $I_0 > 140.77^\circ$, where I is the inclination of the two orbits, because of complications arising from the so-called 'Kozai effect'. The theoretical model is tested against results from numerical integrations of the full equations of motion.

Keywords: Celestial mechanics, stellar dynamics, binaries:general

1. Introduction

In a previous paper (Georgakarakos, 2002), we derived a formula for estimating the eccentricity of the inner binary of a hierarchical triple system with well separated components and initially circular orbits. However, the derivation was based on the assumption that the orbits of the three bodies were on the same plane. In the current paper, we extend the derivation to the more general case of non-coplanar orbits. Generally, the method is the same as in the coplanar regime, although more terms are included in the derivation of the short period equations to improve the accuracy of the model. There are also some minor changes in the calculation of the secular contribution to the eccentricity.

Other recent work on the dynamics of hierarchical triple system includes the work done by Ford et al. (2000), Kiseleva et al. (1998) and Krymowski and Mazeh (1999).

2. Theory

The theoretical model is constructed in the same way as in the coplanar case: we derive expressions for the short period terms by using the definition of the Runge-Lenz vector, while the secular evolution is studied by means of canonical perturbation theory. The combination of the short period and secular part of the eccentricity is achieved by



© 2022 Kluwer Academic Publishers. Printed in the Netherlands.

considering the eccentricity (inner or outer) to consist of a short period and a long period (secular) component, i.e. $e = e_{\text{short}} + e_{\text{sec}}$ (one can picture this by recalling the expansion of the disturbing function in solar system dynamics, where the perturbing potential is given as a sum of an infinite number of cosines of various frequencies). Thus, considering the eccentricity to be initially zero leads to $e_{\text{short}} = -e_{\text{sec}}$ (initially), which implies that, although the eccentricity is initially zero, the short period and secular eccentricity may not be.

2.1. CALCULATION OF THE SHORT-PERIOD CONTRIBUTION TO THE ECCENTRICITY

The equation of motion of the inner binary, using the Jacobi notation (\mathbf{r} for the relative position vector of the inner binary and \mathbf{R} the vector from the centre of mass of m_1 and m_2 to the outer mass m_3), is:

$$\ddot{\mathbf{r}} = -G(m_1 + m_2)\frac{\mathbf{r}}{r^3} + \mathbf{F}, \quad (1)$$

where \mathbf{F} , the perturbation to the inner binary motion, is

$$\begin{aligned} \mathbf{F} = Gm_3 & \left(\frac{\mathbf{R} - \mu_1 \mathbf{r}}{|\mathbf{R} - \mu_1 \mathbf{r}|^3} - \frac{\mathbf{R} + \mu_2 \mathbf{r}}{|\mathbf{R} + \mu_2 \mathbf{r}|^3} \right) = Gm_3 \frac{\partial}{\partial \mathbf{r}} \left(\frac{1}{\mu_1 |\mathbf{R} - \mu_1 \mathbf{r}|} + \right. \\ & \left. + \frac{1}{\mu_2 |\mathbf{R} + \mu_2 \mathbf{r}|} \right) \end{aligned} \quad (2)$$

with

$$\mu_i = \frac{m_i}{m_1 + m_2}, \quad i = 1, 2.$$

Now, since we are dealing with hierarchical triple systems with well separated components, implying that r/R is small, the inverse distances in equation (2) can be expressed as:

$$\frac{1}{|\mathbf{R} - \mu_1 \mathbf{r}|} = \frac{1}{R} \sum_{n=0}^{\infty} \left(\frac{\mu_1 r}{R} \right)^n P_n(\cos \theta)$$

and

$$\frac{1}{|\mathbf{R} + \mu_2 \mathbf{r}|} = \frac{1}{R} \sum_{n=0}^{\infty} \left(-\frac{\mu_2 r}{R} \right)^n P_n(\cos \theta),$$

where P_n are the Legendre polynomials and θ is the angle between the vectors \mathbf{r} and \mathbf{R} . Expanding to third order, the perturbation becomes

$$\begin{aligned} \mathbf{F} = Gm_3 \frac{\partial}{\partial \mathbf{r}} & \left(\frac{3}{2} \frac{(\mathbf{r} \cdot \mathbf{R})^2}{R^5} - \frac{1}{2} \frac{r^2}{R^3} - \frac{5(\mu_2^2 - \mu_1^2)}{2} \frac{(\mathbf{r} \cdot \mathbf{R})^3}{R^7} + \right. \\ & \left. + \frac{3(\mu_2^2 - \mu_1^2)}{2} \frac{r^2 (\mathbf{r} \cdot \mathbf{R})}{R^5} \right). \end{aligned} \quad (3)$$

The first two terms in the above equation come from the quadrupole term (P_2), while the other two come from the octupole term (P_3).

Using now the definition of the Runge-Lenz vector, we can obtain an expression for the inner eccentricity. The inner eccentric vector \mathbf{e}_1 is given by

$$\mathbf{e}_1 = -\frac{\mathbf{r}}{r} + \frac{1}{\mu}(\dot{\mathbf{r}} \times \mathbf{h}), \quad (4)$$

where $\mathbf{h} = \mathbf{r} \times \dot{\mathbf{r}}$ and $\mu = G(m_1 + m_2)$. Assuming that $\mathbf{r} \cdot \dot{\mathbf{r}} = 0$, i.e. the inner binary remains nearly circular (bear in mind that all bodies are on initially circular orbits), differentiating equation (4) and substituting for \mathbf{F} we obtain:

$$\begin{aligned} \dot{\mathbf{e}}_1 = & \frac{Gm_3}{\mu R^3} \left[\left(6 \frac{(\mathbf{r} \cdot \mathbf{R})(\dot{\mathbf{r}} \cdot \mathbf{R})}{R^2} - 15(\mu_2^2 - \mu_1^2) \frac{(\mathbf{r} \cdot \mathbf{R})^2(\dot{\mathbf{r}} \cdot \mathbf{R})}{R^4} + \right. \right. \\ & \left. \left. + 3(\mu_2^2 - \mu_1^2) \frac{r^2(\dot{\mathbf{r}} \cdot \mathbf{R})}{R^2} \right) \mathbf{r} + \left(r^2 - 3 \frac{(\mathbf{r} \cdot \mathbf{R})^2}{R^2} + \frac{15}{2}(\mu_2^2 - \right. \right. \\ & \left. \left. - \mu_1^2) \frac{(\mathbf{r} \cdot \mathbf{R})^3}{R^4} - \frac{9}{2}(\mu_2^2 - \mu_1^2) \frac{r^2(\mathbf{r} \cdot \mathbf{R})}{R^2} \right) \dot{\mathbf{r}} \right]. \quad (5) \end{aligned}$$

Now, choosing a frame of reference such that the initial plane of the inner orbit is our reference plane and the line of nodes is initially on the x-axis, with the positive direction of the x-axis pointing at the ascending node of the outer orbit, the Jacobi vectors can be represented approximately in polar form as $\mathbf{r} = a_1(\cos n_1 t, \sin n_1 t, 0)$ and $\mathbf{R} = a_2(\cos(n_2 t + \phi), \sin(n_2 t + \phi) \cos I, \sin(n_2 t + \phi) \sin I)$, where a_1 and a_2 are the semi-major axes of the inner and outer orbit respectively and ϕ is the initial relative phase of the two binaries. After integrating, the components x_1 and y_1 of the eccentric vector become (expanding the coefficients in powers of $\frac{1}{X}$ and retaining the four leading terms, with X being the period ratio of the two orbits):

$$x_1 = \frac{m_3}{M} \frac{1}{X^2} \left[P_{x21}(t) + \frac{1}{X} P_{x22}(t) + m_* \left(X^{\frac{1}{3}} P_{x31}(t) + \frac{1}{X^{\frac{2}{3}}} P_{x32}(t) \right) \right] + C_{x1} \quad (6)$$

$$y_1 = \frac{m_3}{M} \frac{1}{X^2} \left[P_{y21}(t) + \frac{1}{X} P_{y22}(t) + m_* \left(X^{\frac{1}{3}} P_{y31}(t) + \frac{1}{X^{\frac{2}{3}}} P_{y32}(t) \right) \right] + C_{y1} \quad (7)$$

where $P_i(t)$ are given in the appendix and

$$m_* = \frac{m_2 - m_1}{(m_1 + m_2)^{\frac{2}{3}} M^{\frac{1}{3}}}. \quad (8)$$

M is the total mass of the system and C_{x1} and C_{y1} are constants of integration. The semi-major axes and mean motions were treated as constants in the above calculation.

2.2. CALCULATION OF THE SECULAR CONTRIBUTION TO THE ECCENTRICITY

Secular terms cannot be obtained by the method of Sect. 2.1, because, for an eccentric outer binary, those terms appear as a linear function of time in the expansion of the eccentric vector and therefore, they are valid for limited time. Thus, the secular contribution to the eccentricity is studied by means of the Von Zeipel method.

The doubly averaged over short period terms for both orbits Hamiltonian is (Marchal, 1990, with changes of notation):

$$H = -\frac{Gm_1m_2}{2a_S} - \frac{G(m_1+m_2)m_3}{2a_T} + Q_1 + Q_2, \quad (9)$$

where

$$Q_1 = \frac{1}{8} \frac{Gm_1m_2m_3a_S^2}{(m_1+m_2)a_T^3(1-e_T^2)^{\frac{3}{2}}} [-2 - 3e_S^2 + 3\sin^2 I(1 - e_S^2 + 5e_S^2 \sin^2 g_S)], \quad (10)$$

$$Q_2 = \frac{15Gm_1m_2m_3(m_2-m_1)a_S^3e_Se_T}{64(m_1+m_2)^2a_T^4(1-e_T^2)^{\frac{5}{2}}} [(\sin g_S \sin g_T \cos I + \cos g_S \cos g_T)(4 + 3e_S^2 - 5\sin^2 I(1 - e_S^2 + 7e_S^2 \sin^2 g_S)) - 10(1 - e_S^2) \sin^2 I \cos I \sin g_S \sin g_T]. \quad (11)$$

The subscripts S and T denote the inner and outer longer period orbit respectively. The first term in the Hamiltonian is the Keplerian energy of the inner binary, the second term is the Keplerian energy of the outer binary, while the other two terms represent the interaction between the two binaries. The Q_1 term comes from the P_2 Legendre polynomial and the Q_2 term comes from the P_3 Legendre polynomial. There are also terms which arise from the canonical transformation, but they are of smaller order than the P_3 term.

By using Hamilton's equations (see Marchal, 1990 for the derivation of equations of motion involving the P_2 term), we can now derive the averaged equations of motion of the system (see appendix), which are consistent with the ones in Ford et al. (2000), except that the P_3 term in the Hamiltonian in Ford et al. (2000) has the wrong sign. The same sign error appears in Krymowski and Mazeh (1999). After some exploratory numerical integrations of the five equations of motion of the

system, using a 4th-order Runge-Kutta method with variable stepsize (Press et al., 1996), it became clear that the outer secular eccentricity and the inclination remained almost constant. That, along with the fact that the inner and outer eccentricities were not expected to reach large values (which justifies neglecting powers of x_S , y_S and e_T above the first order) and keeping the dominant term in the equation for \dot{g}_T produced the following simpler system of differential equations:

$$\begin{aligned}\frac{dg_T}{d\tau} &= A \\ \frac{dx_S}{d\tau} &= -By_S + Ce_T \sin g_T \\ \frac{dy_S}{d\tau} &= Dx_S - Ee_T \cos g_T\end{aligned}\quad (12)$$

where

$$\begin{aligned}x_S &= e_S \cos g_S, & y_S &= e_S \sin g_S, \\ A &= \cos I + \frac{1}{2}\beta(4 - 5 \sin^2 I), & B &= 2 - 5 \sin^2 I + \beta \cos I, \\ C &= \frac{5}{16}\alpha \cos I(4 - 15 \sin^2 I), & D &= 2 + \beta \cos I, & E &= \frac{5}{16}\alpha(4 - 5 \sin^2 I), \\ \alpha &= \frac{m_2 - m_1}{m_1 + m_2} \frac{a_S}{a_T}, & \beta &= \frac{m_1 m_2 M^{\frac{1}{2}}}{m_3 (m_1 + m_2)^{\frac{3}{2}}} \left(\frac{a_S}{a_T}\right)^{\frac{1}{2}}, & d\tau &= \frac{3}{4} \frac{G^{\frac{1}{2}} m_3 a_S^{\frac{3}{2}}}{a_T^3 (m_1 + m_2)^{\frac{1}{2}}} dt.\end{aligned}$$

The solution to system (12) is:

$$g_T(\tau) = A\tau + g_{T0} \quad (13)$$

$$\begin{aligned}x_S(\tau) &= K_1 \cos \sqrt{BD}\tau + K_2 \sin \sqrt{BD}\tau + \\ &+ \frac{AC + BE}{BD - A^2} e_T \cos(A\tau + g_{T0})\end{aligned}\quad (14)$$

$$\begin{aligned}y_S(\tau) &= K_1 \sqrt{\frac{D}{B}} \sin \sqrt{BD}\tau - K_2 \sqrt{\frac{D}{B}} \cos \sqrt{BD}\tau + \\ &+ \frac{AE + CD}{BD - A^2} e_T \sin(A\tau + g_{T0}),\end{aligned}\quad (15)$$

where K_1, K_2 are constants of integration and g_{T0} is the initial value of g_T . It should be pointed out here that although the initial outer eccentricity is zero, the secular one is not and consequently an initial outer secular argument of pericentre can be defined. However, the above approximation to secular motion is not valid if $39.23^\circ < I < 140.77^\circ$, since the inner eccentricity is expected to become significant due to

the Kozai effect (Kozai, 1962) and therefore the assumption that the eccentricity remains small is invalid in this case.

2.2.1. Calculation of the initial outer secular eccentricity

As was stated in the previous section, the outer secular eccentricity remains almost constant. Thus, the only thing that remains now is to obtain an estimate for the initial outer secular eccentricity. This can be done in the following way: First, we find an expression for the short period outer eccentricity, by following the same procedure as we did in Sect. (2.1), but this time we do it for the outer orbit. The equation of motion of the outer binary is

$$\ddot{\mathbf{R}} = -GM \left(\mu_1 \frac{\mathbf{R} + \mu_2 \mathbf{r}}{|\mathbf{R} + \mu_2 \mathbf{r}|^3} + \mu_2 \frac{\mathbf{R} - \mu_1 \mathbf{r}}{|\mathbf{R} - \mu_1 \mathbf{r}|^3} \right) \quad (16)$$

and eventually we obtain, to leading order, for the components of the outer short-period eccentric vector:

$$\begin{aligned} x_2 = & \frac{M_*}{X^{\frac{4}{3}}} \left[\cos^2 I \left(\frac{15}{16} \cos(n_2 t + \phi) - \frac{7}{16} \cos(3n_2 t + 3\phi) \right) + \right. \\ & \left. + \frac{7}{16} \cos(3n_2 t + 3\phi) - \frac{3}{16} \cos(n_2 t + \phi) \right] + C_{x_2} \end{aligned} \quad (17)$$

$$\begin{aligned} y_2 = & \frac{M_*}{X^{\frac{4}{3}}} \left[\cos^3 I \left(\frac{21}{16} \sin(n_2 t + \phi) - \frac{7}{16} \sin(3n_2 t + 3\phi) \right) + \right. \\ & \left. + \cos I \left(\frac{7}{16} \sin(3n_2 t + 3\phi) - \frac{9}{16} \sin(n_2 t + \phi) \right) \right] + C_{y_2} \end{aligned} \quad (18)$$

$$\begin{aligned} z_2 = & \frac{M_*}{X^{\frac{4}{3}}} \left[\cos^2 I \sin I \left(\frac{21}{16} \sin(n_2 t + \phi) - \frac{7}{16} \sin(3n_2 t + 3\phi) \right) + \right. \\ & \left. + \sin I \left(\frac{7}{16} \sin(3n_2 t + 3\phi) - \frac{9}{16} \sin(n_2 t + \phi) \right) \right] + C_{z_2}, \end{aligned} \quad (19)$$

$$\text{where } M_* = \frac{m_1 m_2}{(m_1 + m_2)^{\frac{4}{3}} M^{\frac{2}{3}}}. \quad (20)$$

Suppose now that the outer secular eccentric vector is $\mathbf{e}_T = (x_T, y_T, z_T)$. Then, the constants C_{x_2} , C_{y_2} and C_{z_2} in equations (17), (18) and (19) can be replaced by x_T , y_T and z_T , since $\frac{\delta x_T}{\delta x_2} \ll 1$ (same for the pairs $y_T - y_2$ and $z_T - z_2$). Considering that the outer binary is initially circular, i.e. $e_{\text{out}} = 0$, the secular outer eccentric vector will initially be:

$$\mathbf{e}_{T_0} = (x_{T_0}, y_{T_0}, z_{T_0})$$

where

$$x_{T_0} = -\frac{M_*}{X^{\frac{4}{3}}} \left[\cos^2 I \left(\frac{15}{16} \cos \phi - \frac{7}{16} \cos 3\phi \right) + \frac{7}{16} \cos 3\phi - \right.$$

$$-\frac{3}{16} \cos \phi] \quad (21)$$

$$y_{T_0} = -\frac{M^*}{X^{\frac{4}{3}}} [\cos^3 I (\frac{21}{16} \sin \phi - \frac{7}{16} \sin 3\phi) + \cos I (\frac{7}{16} \sin 3\phi - \frac{9}{16} \sin \phi)] \quad (22)$$

$$z_{T_0} = -\frac{M^*}{X^{\frac{4}{3}}} [\cos^2 I \sin I (\frac{21}{16} \sin \phi - \frac{7}{16} \sin 3\phi) + \sin I (\frac{7}{16} \sin 3\phi - \frac{9}{16} \sin \phi)]. \quad (23)$$

$$(24)$$

Thus, the initial outer secular eccentricity is:

$$e_{T_0} = \sqrt{x_{T_0}^2 + y_{T_0}^2 + z_{T_0}^2}. \quad (25)$$

2.3. A FORMULA FOR THE INNER ECCENTRICITY

The expressions that were derived in paragraphs (2.1) and (2.2) for the short period and secular contribution to the inner eccentric vector, can be combined to give an expression for the total eccentricity in the same way we obtained the estimate for the initial outer secular eccentricity, i.e. by replacing the constants in equations (6) and (7) by equations (14) and (15), since the latter evolve on a much larger timescale. This yields (the minus sign in front of x_S and y_S has to do with the orientation of the coordinate system used in Marchal, 1990):

$$x_{in} = x_1 - C_{x_1} - x_S \quad (26)$$

$$y_{in} = y_1 - C_{y_1} - y_S \quad (27)$$

The constants K_1 and K_2 in equations (14) and (15) are determined by the fact that the inner eccentricity is initially zero.

Averaging over time and over the initial relative phase ϕ , the averaged square inner eccentricity will be given by:

$$\begin{aligned} \overline{e_{in}^2} = \langle x_{in}^2 + y_{in}^2 \rangle = & \frac{m_3^2}{M^2} \frac{1}{X^4} \left[\frac{221}{64} - \frac{37}{32} \cos^2 I + \frac{369}{64} \cos^4 I + \right. \\ & + \frac{D}{B} \left(\frac{19}{16} - \frac{5}{2} \cos^2 I + 3 \cos^4 I \right) + \frac{B}{D} \cos^2 I + \frac{1}{X^2} \left[\frac{1011}{144} + \right. \\ & + \frac{471}{24} \cos^2 I + \frac{543}{144} \cos^4 I + \frac{49D}{9B} \cos^2 I + \frac{B}{D} \left(\frac{121}{36} + \right. \\ & \left. \left. + \frac{11}{9} \cos^2 I + \frac{1}{9} \cos^4 I \right) \right] + \frac{1}{X} \left[\frac{45}{3} \cos I + \frac{93}{6} \cos^3 I + \right. \end{aligned}$$

$$\begin{aligned}
& + \frac{D}{B} \left(\frac{7}{6} \cos I + \frac{14}{3} \cos^3 I \right) + \frac{B}{D} \left(\frac{11}{3} \cos I + \frac{2}{3} \cos^3 I \right) + \\
& + m_*^2 X^{\frac{2}{3}} \left[\frac{1275}{8192} + \frac{36525}{8192} \cos^2 I - \frac{103875}{8192} \cos^4 I + \frac{76875}{8192} \cos^6 I + \right. \\
& + \frac{D}{B} \left(\frac{13925}{8192} \cos^2 I - \frac{18875}{4096} \cos^4 I + \frac{25625}{8192} \cos^6 I \right) + \frac{B}{D} \left(\frac{425}{8192} - \right. \\
& - \frac{875}{4096} \cos^2 I + \frac{3125}{8192} \cos^4 I \left. \right) + \frac{m_*^2}{X^{\frac{4}{3}}} \left[\frac{138519}{131072} + \frac{62289}{131072} \cos^2 I + \right. \\
& + \frac{121185}{131072} \cos^4 I + \frac{102375}{131072} \cos^6 I + \frac{D}{B} \left(\frac{54333}{131072} - \frac{42435}{65536} \cos^2 I + \right. \\
& + \frac{119025}{131072} \cos^4 I \left. \right) + \frac{B}{D} \left(\frac{94113}{131072} \cos^2 I - \frac{17955}{65536} \cos^4 I + \right. \\
& + \frac{10125}{131072} \cos^6 I \left. \right) + \frac{m_*^2}{X^{\frac{2}{3}}} \left[\frac{12495}{8192} \cos I - \frac{19875}{4096} \cos^3 I + \right. \\
& + \frac{24375}{8192} \cos^5 I + \frac{D}{B} \left(\frac{25545}{16384} \cos I - \frac{33975}{8192} \cos^3 I + \frac{43125}{16384} \cos^5 I \right) + \\
& + \frac{B}{D} \left(-\frac{555}{16384} \cos I - \frac{5775}{8192} \cos^3 I + \frac{5625}{16384} \cos^5 I \right) \left. \right] - \frac{m_3 m_* M_*}{M X^3} \times \\
& \times \left[\left(\frac{335}{1024} \cos I - \frac{875}{512} \cos I^3 + \frac{1775}{1024} \cos I^5 \right) \left(1 + \frac{D}{B} \right) \frac{AC + BE}{BD - A^2} + \right. \\
& + \left(\frac{155}{1024} \cos I - \frac{335}{512} \cos I^3 + \frac{875}{1024} \cos I^5 \right) \left(1 + \frac{B}{D} \right) \frac{AE + CD}{BD - A^2} \left. \right] - \\
& - \frac{m_3 m_* M_*}{M X^4} \left[\left(\frac{219}{4096} - \frac{1935}{2048} \cos^2 I + \frac{3795}{4096} \cos^4 I \right) \left(1 + \frac{D}{B} \right) \times \right. \\
& \times \frac{AC + BE}{BD - A^2} + \left(\frac{687}{4096} \cos^2 I - \frac{1779}{2048} \cos^4 I + \frac{1575}{4096} \cos^6 I \right) \times \\
& \times \left(1 + \frac{B}{D} \right) \frac{AE + CD}{BD - A^2} \left. \right] + \frac{M_*^2}{X^{\frac{8}{3}}} \left[\frac{(AC + BE)^2}{(BD - A^2)^2} \left(1 + \frac{D}{B} \right) \left(\frac{29}{512} - \right. \right. \\
& - \frac{47}{256} \cos^2 I + \frac{137}{512} \cos^4 I \left. \right) + \frac{(AE + CD)^2}{(BD - A^2)^2} \left(1 + \frac{B}{D} \right) \times \\
& \times \left(\frac{65}{512} \cos^2 I - \frac{119}{256} \cos^4 I + \frac{245}{512} \cos^6 I \right) \left. \right] + \frac{1}{2} \frac{M_*^2}{X^{\frac{8}{3}}} \times \\
& \times \left[\frac{(AC + BE)^2}{(BD - A^2)^2} + \frac{(AE + CD)^2}{(BD - A^2)^2} \right] \left(\frac{29}{256} - \frac{29}{256} \cos^2 I - \right. \\
& - \frac{101}{256} \cos^4 I + \frac{245}{256} \cos^6 I \left. \right). \tag{28}
\end{aligned}$$

The above formula is expected to be rather inaccurate in situations where the system parameters yield very small values for the quantity $BD - A^2$, i.e. when we are near to a secular resonance. Although the quantities \sqrt{BD} and A are approximations to the secular frequencies of

the inner and outer arguments of pericentre respectively, the solution of $BD - A^2 = 0$, which reduces to

$$3(1 - 3 \sin^2 I)(1 - \beta^2) - \frac{25}{4}\beta^2 \sin^4 I = 0, \quad (29)$$

could roughly identify the location of the secular resonance. However, in order to get a more accurate solution to the problem, the inclusion of more terms is necessary in system (12) or in the averaged Hamiltonian.

3. Comparison with numerical results

In order to test the range of applicability of the theory developed in the previous sections, we integrated the full equations of motion numerically, using a symplectic integrator with time transformation (Mikkola, 1997).

The code calculates the relative position and velocity vectors of the two binaries at every time step. Then, by using standard two body formulae, we computed the orbital elements of the two binaries. Integrations were arranged such that the writing index Iwr was 1, the average number of steps per inner binary period NS was 60, the method coefficients $a1$ and $a2$ were 1 and 15 respectively and the correction index $icor$ was 1. In all simulations, we confined ourselves to systems with mass ratios within the range 10 : 1 since, “among stellar triples, mass ratios are rare outside a range of approximately 10 : 1, although such systems would be inherently difficult to recognise” (Eggleton and Kiseleva, 1995); and initial period ratio $X \geq 10$. We also used units such that $G = 1$ and $m_1 + m_2 = 1$ and we always started the integrations with $a_1 = 1$. In that system of units, the initial conditions for the numerical integrations were as follows:

$$\begin{aligned} r_1 &= 1, & r_2 &= 0, & r_3 &= 0 \\ R_1 &= a_2 \cos \phi, & R_2 &= a_2 \sin \phi \cos I, & R_3 &= a_2 \sin \phi \sin I \\ \dot{r}_1 &= 0, & \dot{r}_2 &= 1, & \dot{r}_3 &= 0 \\ \dot{R}_1 &= -\sqrt{\frac{M}{a_2}} \sin \phi, & \dot{R}_2 &= \sqrt{\frac{M}{a_2}} \cos \phi \cos I, & \dot{R}_3 &= \sqrt{\frac{M}{a_2}} \cos \phi \sin I, \end{aligned}$$

where \mathbf{r} and \mathbf{R} are the relative position vectors of the inner and outer orbit respectively.

3.1. SHORT PERIOD EFFECTS

First we tested the validity of equations (6) and (7). The integrations and comparison with the analytical results were done for $\phi = 90^\circ$, i.e. the outer binary was ahead of the inner one at right angles. However, this does not affect the qualitative understanding of the problem at all.

These results are presented in Table 1, which gives the percentage error between the averaged, over time, numerical and theoretical e_{in} (the theoretical eccentricity was obtained by evaluating equations (6) and (7) everytime we had an output from the symplectic integrator; both averaged numerical and theoretical eccentricities were calculated by using the trapezium rule). The integrations were performed over one outer orbital period time span (in our system of units, the initial outer orbital period is $T_{\text{out}} = 2\pi X_0$, where X_0 is the initial period ratio). For each pair (m_3, X_0) in Table 1, there are five entries, corresponding, from top to bottom, to the following inner binaries: $m_1 = 0.1 - m_2 = 0.9$, $m_1 = 0.2 - m_2 = 0.8$, $m_1 = 0.3 - m_2 = 0.7$, $m_1 = 0.4 - m_2 = 0.6$ and $m_1 = 0.5 - m_2 = 0.5$. A dash in Table 1 denotes that the analogy among the masses was outside the range 10 : 1. The inclination of the two orbits is $I = 20^\circ$.

Most of the results show a rather significant error for systems with strong perturbation to the inner binary (small X_0 -large m_3). However, the error drops considerably as we move to larger values of X_0 (the error becomes less than 10% for all systems with $X_0 \geq 20$). This is consistent with our aim to obtain a reasonable model for the evolution of the inner eccentricity in hierarchical triple systems with well separated components. One should bear in mind that a period ratio of 20 is close to the lower boundary for observed hierarchical triple systems. Fig.1, which is a plot of inner eccentricity against time, demonstrates the good agreement between the theory (dashed curve) and the numerical results (continuous curve). The parameters of the system are: $m_1 = 0.4$, $m_3 = 4$, $X_0 = 20$, $I = 20^\circ$, $\phi = 90^\circ$ and the integration time span is one outer orbital period ($T_{\text{out}} = 125.6$).

3.2. SHORT AND LONG PERIOD EFFECTS

Next, we tested equation (28), which accounts for the short period and secular effects to the inner eccentricity. The formula was compared with results obtained from integrating the full equations of motion numerically. These results are presented in Table 2, which gives the percentage error between the averaged, over time and initial phase ϕ , numerical e_{in}^2 and equation (28). In the case of a system with noticeable secular evolution, the error is accompanied by the period of the long oscillation of the eccentricity, which is the same as the integration time

Table I. Percentage error between the averaged numerical and averaged theoretical e_{in} . The theoretical model is based on equations (6) and (7). For all systems, $I = 20^\circ$ and $\phi = 90^\circ$. Each line corresponds to a different inner binary pair (0.1 – 0.9, 0.2 – 0.8, 0.3 – 0.7, 0.4 – 0.6 and 0.5 – 0.5). A dash denotes that the mass ratio is outside the range 10 : 1.

| $m_3 \setminus X_0$ | 10 | 15 | 20 | 25 | 30 | 50 |
|---------------------|------|------|-----|-----|-----|-----|
| 0.05 | - | - | - | - | - | - |
| | - | - | - | - | - | - |
| | - | - | - | - | - | - |
| | - | - | - | - | - | - |
| 0.09 | 5.5 | 2.6 | 1.5 | 1 | 0.7 | 0.3 |
| | 5.1 | 2.5 | 1.6 | 1.1 | 0.9 | 0.4 |
| | 5.6 | 2.7 | 1.7 | 1.2 | 0.9 | 0.4 |
| | 5.9 | 2.8 | 1.7 | 1.2 | 0.9 | 0.4 |
| | 6.1 | 2.9 | 1.8 | 1.2 | 0.9 | 0.4 |
| | 6.2 | 3 | 1.8 | 1.2 | 0.9 | 0.4 |
| 0.5 | 10 | 5.4 | 3.6 | 2.7 | 2.1 | 1.2 |
| | 10.4 | 5.5 | 3.6 | 2.6 | 2.1 | 1.1 |
| | 10.7 | 5.6 | 3.6 | 2.6 | 2 | 1 |
| | 11 | 5.7 | 3.7 | 2.7 | 2.1 | 1 |
| | 11.2 | 5.9 | 3.8 | 2.8 | 2.2 | 1.1 |
| | 1 | 13.9 | 7.5 | 5 | 3.7 | 3 |
| 14.2 | | 7.6 | 5 | 3.7 | 2.9 | 1.6 |
| 14.5 | | 7.7 | 5 | 3.7 | 2.8 | 1.5 |
| 14.7 | | 7.9 | 5.1 | 3.7 | 2.9 | 1.5 |
| 15 | | 8.1 | 5.3 | 3.9 | 3 | 1.6 |
| 1.5 | | - | - | - | - | - |
| | 16.7 | 8.9 | 5.9 | 4.3 | 3.4 | 1.8 |
| | 16.9 | 9 | 5.9 | 4.3 | 3.4 | 1.8 |
| | 17.3 | 9.3 | 6 | 4.4 | 3.4 | 1.8 |
| | 17.7 | 9.5 | 6.3 | 4.6 | 3.6 | 1.9 |
| | 2 | - | - | - | - | - |
| 18.5 | | 9.9 | 6.5 | 4.8 | 3.7 | 2 |
| 18.7 | | 10 | 6.5 | 4.8 | 3.7 | 1.9 |
| 19 | | 10.2 | 6.7 | 4.9 | 3.8 | 2 |
| 19.4 | | 10.4 | 6.9 | 5.1 | 4 | 2.1 |
| 2.6 | | - | - | - | - | - |
| | - | - | - | - | - | - |
| | 20.2 | 10.8 | 7 | 5.2 | 4 | 2.1 |
| | 20.6 | 11 | 7.2 | 5.3 | 4.1 | 2.1 |
| | 21 | 11.3 | 7.5 | 5.5 | 4.3 | 2.2 |
| | 3 | - | - | - | - | - |
| - | | - | - | - | - | - |
| 21 | | 11.2 | 7.3 | 5.4 | 4.2 | 2.2 |
| 21.4 | | 11.5 | 7.5 | 5.4 | 4.3 | 2.2 |
| 21.8 | | 11.7 | 7.7 | 5.7 | 4.4 | 2.3 |
| 3.4 | | - | - | - | - | - |
| | - | - | - | - | - | - |
| | - | - | - | - | - | - |
| | 22 | 11.8 | 7.7 | 5.6 | 4.4 | 2.3 |
| | 22.4 | 12.1 | 8 | 5.8 | 4.6 | 2.4 |
| | 4 | - | - | - | - | - |
| - | | - | - | - | - | - |
| - | | - | - | - | - | - |
| 22.9 | | 12.2 | 8 | 5.8 | 4.6 | 2.3 |
| 23.2 | | 12.5 | 8.3 | 6 | 4.7 | 2.5 |
| 4.5 | | - | - | - | - | - |
| | - | - | - | - | - | - |
| | - | - | - | - | - | - |
| | - | - | - | - | - | - |
| | 23.8 | 12.8 | 8.4 | 6.2 | 4.8 | 2.5 |
| | 5 | - | - | - | - | - |
| - | | - | - | - | - | - |
| - | | - | - | - | - | - |
| - | | - | - | - | - | - |
| 24.2 | | 13 | 8.6 | 6.3 | 4.9 | 2.6 |

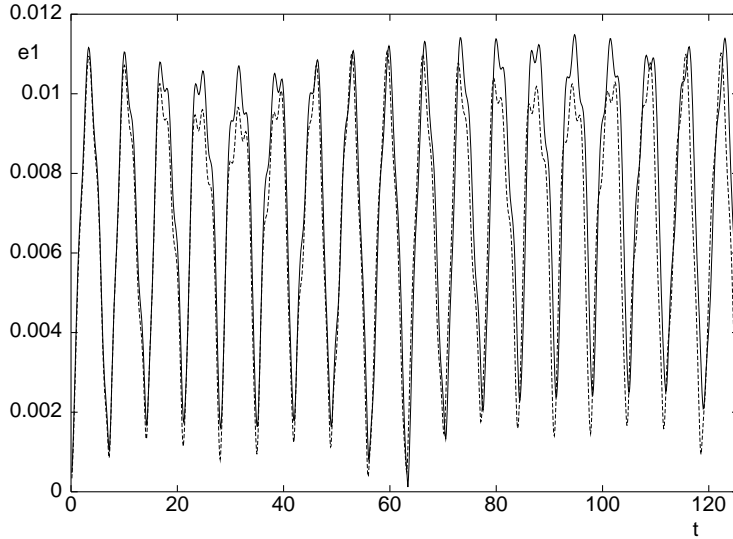


Figure 1. Inner eccentricity against time for a system with $m_1 = 0.4$, $m_3 = 4$, $X_0 = 20$, $I = 20^\circ$ and $\phi = 90^\circ$. The integration time span is one outer orbital period ($T_{\text{out}} = 125.6$). The continuous curve comes from the numerical integration of the full equations of motion, while the dashed curve is a plot of equations (6) and (7). In the system of units used, the inner binary period is $T_{\text{in}} = 2\pi$.

span, while the rest of the systems were integrated over one outer orbital period (denoted by a dash), since there was not any noticeable secular evolution when those systems were integrated over longer time spans. For each pair (m_3, X_0) in Table 2, there are three pairs of entries, corresponding, from top to bottom, to 10° , 20° and 30° inclination. A negative entry means that formula (28) is an overestimate to the numerical result. Each system was numerically integrated for $\phi = 0^\circ - 360^\circ$ with a step of 45° . After the end of each simulation, e_{in}^2 was averaged over time using the trapezium rule and after the integrations for all ϕ were done, we averaged over the relative initial phase by using the rectangle rule. The integrations were also done for smaller steps in ϕ (10° , 1° and 0.1°), but there was not any difference in the outcome. All the integrations presented in Table 2 were done for $m_1 = 0.2$ and $m_2 = 0.8$, but similar results are expected for the other inner binary mass ratios.

For systems with $m_3 = 0.09$, there is a significant discrepancy between the numerical results and the theoretical model. This is clearly demonstrated in Figs. 2 and 3. It is easily noted in Fig. 3, which is a plot based on equations (26) and (27), that the long period and amplitude of the oscillation are larger than the ones obtained from the numerical integrations (Fig. 2). This is due to the fact that the system

is in the vicinity of a secular resonance, i.e. the secular frequencies of the two arguments of pericentre are nearly equal and where, as stated in section(2.3), the secular part of our theory is not expected to work very well. The effect of the resonance gets less significant as we move away from the solution of $\sqrt{BD} - A = 0$. However, for systems with $m_1 = m_2$ there is no such concern, since the long term evolution of the system is independent of the outer argument of pericentre g_T , as can be seen in Sect. (2.2).

The rest of the numerical results are generally in good agreement with our theory. The error is just above or drops under 10% for all masses and inclinations with $X \geq 15$. Similar results are expected for other inner mass ratios.

4. Conclusion

We have extended the method of getting an estimate for the inner eccentricity in hierarchical triple systems on initially circular orbits to situations where the stars are in non-coplanar orbits. Again, the equations developed throughout this paper, give reasonable results for the parameter ranges discussed. The addition of two more terms in the equations for short term evolution has made our theoretical model more accurate, especially for systems where the perturbation to the inner binary is rather strong (the equations in the coplanar case only include the dominant P_2 and P_3 terms). Our future aim is to complete that type of calculation by deriving a formula for systems with eccentric outer binaries.

Appendix

A.

Short period components of the eccentric vector:

$$\begin{aligned}
 P_{x21}(t) = & \frac{11}{8} \cos n_1 t + \frac{1}{8} \cos 3n_1 t + \frac{3}{16} \cos ((n_1 - 2n_2)t - 2\phi) + \\
 & + \frac{3}{16} \cos ((n_1 + 2n_2)t + 2\phi) + \frac{1}{16} \cos ((3n_1 - 2n_2)t - 2\phi) + \\
 & + \frac{1}{16} \cos ((3n_1 + 2n_2)t + 2\phi) + \cos I \left[\frac{9}{8} \cos ((n_1 - 2n_2)t - 2\phi) - \right. \\
 & \left. - \frac{9}{8} \cos ((n_1 + 2n_2)t + 2\phi) + \frac{1}{8} \cos ((3n_1 - 2n_2)t - 2\phi) - \right.
 \end{aligned}$$

Table II. Percentage error between the averaged numerical e_{in}^2 and equation (28) for systems with $m_1 = 0.2$ and $m_2 = 0.8$. The error is accompanied by the integration time span. A dash denotes that the system was integrated for one outer orbital period. For each $m_3 - X_0$ pair we have three entries corresponding, from top to bottom, to an inclination of 10° , 20° and 30° respectively.

| $m_3 \setminus X_0$ | 10 | 15 | 20 | 25 | 30 | 50 |
|---------------------|---------|--------|--------|--------|--------|---------|
| 0.09 | -219.8 | -51.3 | -20.6 | -12 | -6.6 | -0.7 |
| | 24000 | 62000 | 105000 | 160000 | 215000 | 510000 |
| | -245.1 | -50.3 | -21.5 | -9.3 | -5.9 | 0.3 |
| | 33500 | 81000 | 142000 | 200000 | 280000 | 650000 |
| | -1383.8 | -396.3 | -75.5 | -33.9 | -15.8 | -2.6 |
| | 80000 | 210000 | 350000 | 550000 | 700000 | 1640000 |
| 0.5 | 14.6 | 7.1 | 3.8 | 2.8 | 1.8 | 0.1 |
| | - | - | - | 3500 | 5200 | 15000 |
| | 12.5 | 6.3 | 3.7 | 2.3 | 1.5 | -0.1 |
| | 550 | 1400 | 2400 | 4100 | 6000 | 17000 |
| | 8.2 | 2.8 | 1.5 | 0.7 | 0.1 | -0.4 |
| | 650 | 1800 | 3200 | 5200 | 7800 | 22500 |
| 1 | 19.4 | 10.9 | 7.3 | 5.3 | 4.1 | 2.4 |
| | - | - | - | - | - | 10000 |
| | 14.8 | 8.2 | 5.5 | 4.2 | 3.2 | 1.6 |
| | - | 900 | 1800 | 2700 | 4200 | 12200 |
| | 7.4 | 3.2 | 1.6 | 0.9 | 0.3 | 0.1 |
| | 450 | 1100 | 2100 | 3400 | 5200 | 15000 |
| 1.5 | 22 | 12.5 | 8.6 | 6.5 | 5.1 | 3 |
| | - | - | - | - | - | 9000 |
| | 16.8 | 9 | 6.4 | 4.9 | 3.9 | 2 |
| | - | 800 | 1400 | 2200 | 3400 | 9900 |
| | 8.7 | 2.3 | 1 | 0.8 | -0.1 | -0.4 |
| | 300 | 900 | 1800 | 2800 | 4400 | 13000 |
| 2 | 23.7 | 13.4 | 9.2 | 7 | 5.7 | 3.1 |
| | - | - | - | - | - | - |
| | 18.1 | 9.8 | 6.8 | 5.1 | 4.2 | 2.2 |
| | - | 600 | 1250 | 2000 | 3000 | 9000 |
| | 8.1 | 2.6 | 0.8 | 0.7 | 0.1 | 0.1 |
| | 300 | 800 | 1600 | 2500 | 3800 | 11000 |

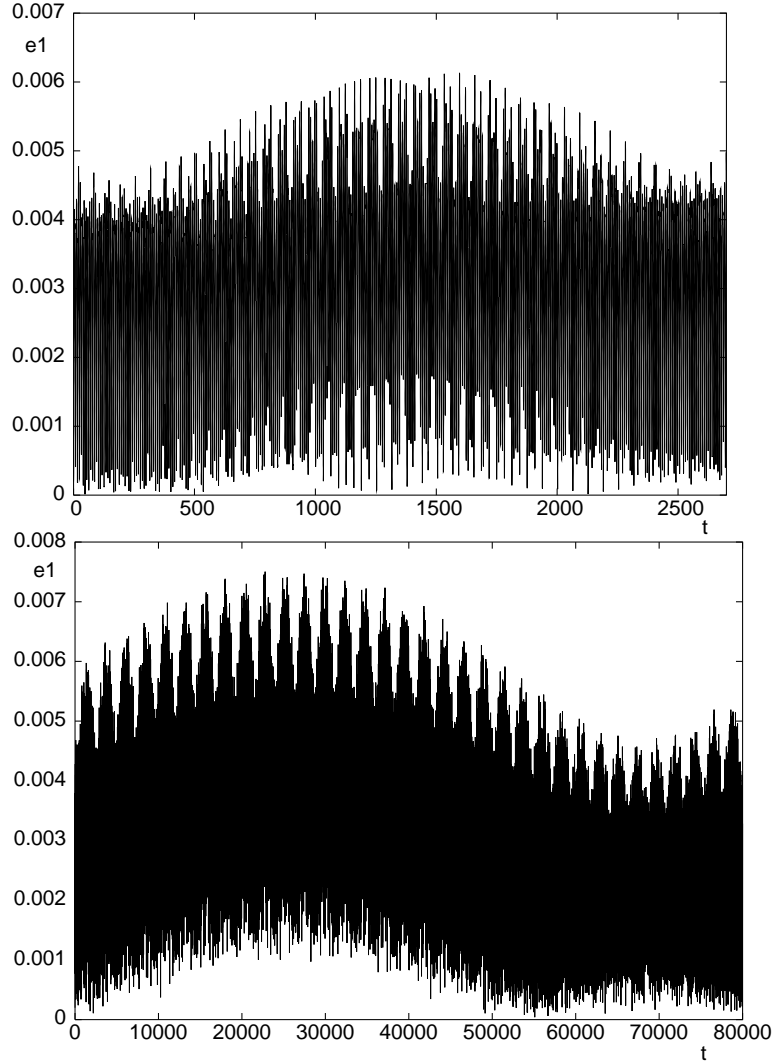


Figure 2. Secular resonance for a system with $m_1 = 0.2$, $m_3 = 0.09$, $X_0 = 10$, $I = 30^\circ$ and $\phi = 90^\circ$. The outer orbital period is $T_{\text{out}} = 62.8$. The graphs come from the numerical integration of the full equations of motion. The top graph is a magnification of the first peak of the bottom graph.

$$\begin{aligned}
& -\frac{1}{8} \cos((3n_1 + 2n_2)t + 2\phi)] + \cos^2 I \left[-\frac{15}{8} \cos n_1 t - \frac{1}{8} \cos 3n_1 t + \right. \\
& + \frac{15}{16} \cos((n_1 - 2n_2)t - 2\phi) + \frac{15}{16} \cos((n_1 + 2n_2)t + 2\phi) + \\
& \left. + \frac{1}{16} \cos((3n_1 - 2n_2)t - 2\phi) + \frac{1}{16} \cos((3n_1 + 2n_2)t + 2\phi) \right] \quad (30)
\end{aligned}$$

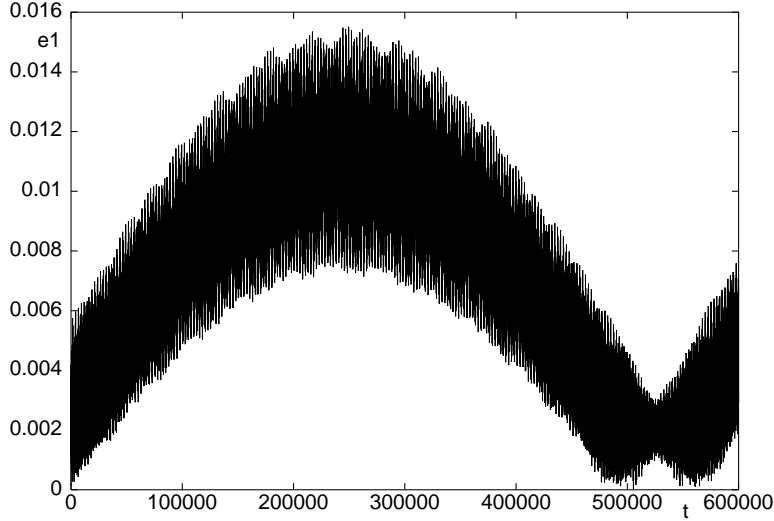


Figure 3. Secular resonance for a system with $m_1 = 0.2$, $m_3 = 0.09$, $X_0 = 10$, $I = 30^\circ$ and $\phi = 90^\circ$ based on equations (26) and (27). The outer orbital period is $T_{\text{out}} = 62.8$. Note the long period and large amplitude of the oscillation.

$$\begin{aligned}
P_{x22}(t) = & \frac{3}{8} \cos((n_1 - 2n_2)t - 2\phi) - \frac{3}{8} \cos((n_1 + 2n_2)t + 2\phi) + \\
& + \frac{1}{24} \cos((3n_1 - 2n_2)t - 2\phi) - \frac{1}{24} \cos((3n_1 + 2n_2)t + 2\phi) + \\
& + \cos I \left[\frac{9}{4} \cos((n_1 - 2n_2)t - 2\phi) + \frac{9}{4} \cos((n_1 + 2n_2)t + 2\phi) + \right. \\
& + \left. \frac{1}{12} \cos((3n_1 - 2n_2)t - 2\phi) + \frac{1}{12} \cos((3n_1 + 2n_2)t + 2\phi) \right] + \\
& + \cos^2 I \left[\frac{15}{8} \cos((n_1 - 2n_2)t - 2\phi) - \frac{15}{8} \cos((n_1 + 2n_2)t + 2\phi) + \right. \\
& + \left. \frac{1}{24} \cos((3n_1 - 2n_2)t - 2\phi) - \frac{1}{24} \cos((3n_1 + 2n_2)t + 2\phi) \right] \quad (31)
\end{aligned}$$

$$\begin{aligned}
P_{x31}(t) = & \cos I \left[\frac{25}{64} \cos(3n_2t + 3\phi) - \frac{165}{64} \cos(n_2t + \phi) \right] + \\
& + \cos^3 I \left[\frac{225}{64} \cos(n_2t + \phi) - \frac{25}{64} \cos(3n_2 + 3\phi) \right] \quad (32)
\end{aligned}$$

$$\begin{aligned}
P_{x32}(t) = & -\frac{69}{128} \cos((2n_1 - n_2)t - \phi) - \frac{69}{128} \cos((2n_1 + n_2)t + \phi) - \\
& -\frac{15}{128} \cos((2n_1 - 3n_2)t - 3\phi) - \frac{15}{128} \cos((2n_1 + 3n_2)t + 3\phi) - \\
& -\frac{45}{512} \cos((4n_1 - n_2)t - \phi) - \frac{45}{512} \cos((4n_1 + n_2)t + \phi) - \\
& -\frac{15}{512} \cos((4n_1 - 3n_2)t - 3\phi) - \frac{15}{512} \cos((4n_1 + 3n_2)t + 3\phi) +
\end{aligned}$$

$$\begin{aligned}
& + \cos I \left[-\frac{21}{32} \cos((2n_1 - n_2)t - \phi) + \frac{21}{32} \cos((2n_1 + n_2)t + \phi) - \right. \\
& - \frac{15}{32} \cos((2n_1 - 3n_2)t - 3\phi) + \frac{15}{32} \cos((2n_1 + 3n_2)t + 3\phi) - \\
& - \frac{45}{512} \cos((4n_1 - n_2)t - \phi) + \frac{45}{512} \cos((4n_1 + n_2)t + \phi) - \\
& - \left. \frac{45}{512} \cos((4n_1 - 3n_2)t - 3\phi) + \frac{45}{512} \cos((4n_1 + 3n_2)t + 3\phi) \right] + \\
& + \cos^2 I \left[\frac{75}{128} \cos((2n_1 - n_2)t - \phi) + \frac{75}{128} \cos((2n_1 + n_2)t + \phi) - \right. \\
& - \frac{75}{128} \cos((2n_1 - 3n_2)t - 3\phi) - \frac{75}{128} \cos((2n_1 + 3n_2)t + 3\phi) + \\
& + \frac{45}{512} \cos((4n_1 - n_2)t - \phi) + \frac{45}{512} \cos((4n_1 + n_2)t + \phi) - \\
& - \left. \frac{45}{512} \cos((4n_1 - 3n_2)t - 3\phi) - \frac{45}{512} \cos((4n_1 + 3n_2)t + 3\phi) \right] + \\
& + \cos^3 I \left[\frac{45}{64} \cos((2n_1 - n_2)t - \phi) - \frac{45}{64} \cos((2n_1 + n_2)t + \phi) - \right. \\
& - \frac{15}{64} \cos((2n_1 - 3n_2)t - 3\phi) + \frac{15}{64} \cos((2n_1 + 3n_2)t + 3\phi) + \\
& + \frac{45}{512} \cos((4n_1 - n_2)t - \phi) - \frac{45}{512} \cos((4n_1 + n_2)t + \phi) - \\
& - \left. \frac{15}{512} \cos((4n_1 - 3n_2)t - 3\phi) + \frac{15}{512} \cos((4n_1 + 3n_2)t + 3\phi) \right] \quad (33)
\end{aligned}$$

$$\begin{aligned}
P_{y21}(t) = & -\frac{7}{8} \sin n_1 t + \frac{1}{8} \sin 3n_1 t - \frac{15}{16} \sin((n_1 - 2n_2)t - 2\phi) - \\
& - \frac{15}{16} \sin((n_1 + 2n_2)t + 2\phi) + \frac{1}{16} \sin((3n_1 - 2n_2)t - 2\phi) + \\
& + \frac{1}{16} \sin((3n_1 + 2n_2)t + 2\phi) + \cos I \left[-\frac{9}{8} \sin((n_1 - 2n_2)t - 2\phi) + \right. \\
& + \frac{9}{8} \sin((n_1 + 2n_2)t + 2\phi) + \frac{1}{8} \sin((3n_1 - 2n_2)t - 2\phi) - \\
& - \left. \frac{1}{8} \sin((3n_1 + 2n_2)t + 2\phi) \right] + \cos^2 I \left[\frac{3}{8} \sin n_1 t - \frac{1}{8} \sin 3n_1 t - \right. \\
& - \frac{3}{16} \sin((n_1 - 2n_2)t - 2\phi) - \frac{3}{16} \sin((n_1 + 2n_2)t + 2\phi) + \\
& + \left. \frac{1}{16} \sin((3n_1 - 2n_2)t - 2\phi) + \frac{1}{16} \sin((3n_1 + 2n_2)t + 2\phi) \right] \quad (34)
\end{aligned}$$

$$\begin{aligned}
P_{y22}(t) = & -\frac{15}{8} \sin((n_1 - 2n_2)t - 2\phi) + \frac{15}{8} \sin((n_1 + 2n_2)t + 2\phi) + \\
& + \frac{1}{24} \sin((3n_1 - 2n_2)t - 2\phi) - \frac{1}{24} \sin((3n_1 + 2n_2)t + 2\phi) +
\end{aligned}$$

$$\begin{aligned}
& + \cos I \left[-\frac{9}{4} \sin((n_1 - 2n_2)t - 2\phi) - \frac{9}{4} \sin((n_1 + 2n_2)t + 2\phi) + \right. \\
& + \frac{1}{12} \sin((3n_1 - 2n_2)t - 2\phi) + \frac{1}{12} \sin((3n_1 + 2n_2)t + 2\phi) \left. \right] + \\
& + \cos^2 I \left[-\frac{3}{8} \sin((n_1 - 2n_2)t - 2\phi) + \frac{3}{8} \sin((n_1 + 2n_2)t + 2\phi) + \right. \\
& + \frac{1}{24} \sin((3n_1 - 2n_2)t - 2\phi) - \frac{1}{24} \sin((3n_1 + 2n_2)t + 2\phi) \left. \right] \quad (35)
\end{aligned}$$

$$\begin{aligned}
P_{y31}(t) & = \frac{25}{64} \sin(3n_2t + 3\phi) - \frac{15}{64} \sin(n_2t + \phi) + \\
& + \cos^2 I \left[\frac{75}{64} \sin(n_2t + \phi) - \frac{25}{64} \sin(3n_2 + 3\phi) \right] \quad (36)
\end{aligned}$$

$$\begin{aligned}
P_{y32}(t) & = \frac{33}{64} \sin((2n_1 - n_2)t - \phi) + \frac{33}{64} \sin((2n_1 + n_2)t + \phi) + \\
& + \frac{15}{64} \sin((2n_1 - 3n_2)t - 3\phi) + \frac{15}{64} \sin((2n_1 + 3n_2)t + 3\phi) - \\
& - \frac{45}{512} \sin((4n_1 - n_2)t - \phi) - \frac{45}{512} \sin((4n_1 + n_2)t + \phi) - \\
& - \frac{15}{512} \sin((4n_1 - 3n_2)t - 3\phi) - \frac{15}{512} \sin((4n_1 + 3n_2)t + 3\phi) + \\
& + \cos I \left[\frac{51}{128} \sin((2n_1 - n_2)t - \phi) - \frac{51}{128} \sin((2n_1 + n_2)t + \phi) + \right. \\
& + \frac{75}{128} \sin((2n_1 - 3n_2)t - 3\phi) - \frac{75}{128} \sin((2n_1 + 3n_2)t + 3\phi) - \\
& - \frac{45}{512} \sin((4n_1 - n_2)t - \phi) + \frac{45}{512} \sin((4n_1 + n_2)t + \phi) - \\
& - \frac{45}{512} \sin((4n_1 - 3n_2)t - 3\phi) + \frac{45}{512} \sin((4n_1 + 3n_2)t + 3\phi) \left. \right] + \\
& + \cos^2 I \left[-\frac{15}{32} \sin((2n_1 - n_2)t - \phi) - \frac{15}{32} \sin((2n_1 + n_2)t + \phi) + \right. \\
& + \frac{15}{32} \sin((2n_1 - 3n_2)t - 3\phi) + \frac{15}{32} \sin((2n_1 + 3n_2)t + 3\phi) + \\
& + \frac{45}{512} \sin((4n_1 - n_2)t - \phi) + \frac{45}{512} \sin((4n_1 + n_2)t + \phi) - \\
& - \frac{45}{512} \sin((4n_1 - 3n_2)t - 3\phi) - \frac{45}{512} \sin((4n_1 + 3n_2)t + 3\phi) \left. \right] + \\
& + \cos^3 I \left[-\frac{45}{128} \sin((2n_1 - n_2)t - \phi) + \frac{45}{128} \sin((2n_1 + n_2)t + \phi) + \right. \\
& + \frac{15}{128} \sin((2n_1 - 3n_2)t - 3\phi) - \frac{15}{128} \sin((2n_1 + 3n_2)t + 3\phi) + \\
& + \frac{45}{512} \sin((4n_1 - n_2)t - \phi) - \frac{45}{512} \sin((4n_1 + n_2)t + \phi) -
\end{aligned}$$

$$-\frac{15}{512} \sin((4n_1 - 3n_2)t - 3\phi) + \frac{15}{512} \sin((4n_1 + 3n_2)t + 3\phi) \quad (37)$$

The complete secular equations of motion:

$$\begin{aligned} \frac{dx_S}{d\tau} = & \frac{5}{(1 - e_T^2)^{\frac{3}{2}}} \sin^2 I \frac{1 - x_S^2}{(1 - x_S^2 - y_S^2)^{\frac{1}{2}}} y_S + \frac{5}{16} \alpha \frac{e_T}{(1 - e_T^2)^{\frac{5}{2}}} (1 - x_S^2 - \\ & - y_S^2)^{\frac{1}{2}} [\sin g_T \cos I (4 + 3(x_S^2 + y_S^2)) - 5 \sin^2 I (1 - x_S^2 + 6y_S^2)) - \\ & - 10(1 - x_S^2 - y_S^2) \sin I^2 \cos I \sin g_T + 2(3 + 5 \sin^2 I)(y_S^2 \sin g_T \times \\ & \times \cos I + x_S y_S \cos g_T) + 20 \sin^2 I \cos I y_S^2 \sin g_T - 70 \sin^2 I (y_S^2 \times \\ & \times \sin g_T \cos I + x_S y_S \cos g_T)] + \frac{5}{16} \alpha \beta \frac{e_T}{(1 - e_T^2)^3} [y_S^2 \sin g_T (4 + \\ & + 3(x_S^2 + y_S^2)) - 5 \sin^2 I (1 - x_S^2 + 6y_S^2)) + 10 \cos I (y_S^2 \sin g_T \times \\ & \times \cos I + x_S y_S \cos g_T) (1 - x_S^2 + 6y_S^2) + 10(1 - x_S^2 - y_S^2) y_S^2 \times \\ & \times \sin g_T (2 \cos^2 I - \sin^2 I)] + \frac{5}{16} \alpha \frac{e_T}{(1 - e_T^2)^{\frac{5}{2}}} \frac{1}{(1 - x_S^2 - y_S^2)^{\frac{1}{2}}} \times \\ & \times [y_S^2 \sin g_T \cos I (4 + 3(x_S^2 + y_S^2)) - 5 \sin^2 I (1 - x_S^2 + 6y_S^2)) + \\ & + 10(y_S^2 \sin g_T \cos I + x_S y_S \cos g_T) \cos^2 I (1 - x_S^2 + 6y_S^2) + \\ & + 10(1 - x_S^2 - y_S^2) y_S^2 \sin g_T (2 \cos^2 I - \sin^2 I) \cos I] - \\ & - \frac{\beta}{(1 - e_T^2)^2} y_S \cos I (1 - x_S^2 + 4y_S^2) - \frac{1}{(1 - e_T^2)^{\frac{3}{2}}} y_S \times \\ & \times \frac{2 - 2x_S^2 + 3y_S^2}{(1 - x_S^2 - y_S^2)^{\frac{1}{2}}} \end{aligned} \quad (38)$$

$$\begin{aligned} \frac{dy_S}{d\tau} = & -\frac{5}{(1 - e_T^2)^{\frac{3}{2}}} \sin^2 I \frac{x_S y_S^2}{(1 - x_S^2 - y_S^2)^{\frac{1}{2}}} y_S + \frac{5}{16} \alpha \frac{e_T}{(1 - e_T^2)^{\frac{5}{2}}} (1 - \\ & - x_S^2 - y_S^2)^{\frac{1}{2}} [-\cos g_T (4 + 3(x_S^2 + y_S^2)) - 5 \sin^2 I (1 - x_S^2 + \\ & + 6y_S^2)) - 2(3 + 5 \sin^2 I)(x_S y_S \sin g_T \cos I + x_S^2 \cos g_T) - \\ & - 20 \sin^2 I \cos I x_S y_S \sin g_T] + \frac{5}{16} \alpha \beta \frac{e_T}{(1 - e_T^2)^3} [-x_S y_S \sin g_T \times \\ & \times (4 + 3(x_S^2 + y_S^2)) - 5 \sin^2 I (1 - x_S^2 + 6y_S^2)) - 10 \cos I (x_S \times \\ & \times y_S \sin g_T \cos I + x_S^2 \cos g_T) (1 - x_S^2 + 6y_S^2) - 10(1 - x_S^2 - \\ & - y_S^2) x_S y_S \sin g_T (2 \cos^2 I - \sin^2 I)] + \frac{5}{16} \alpha \frac{e_T}{(1 - e_T^2)^{\frac{5}{2}}} \times \\ & \times \frac{1}{(1 - x_S^2 - y_S^2)^{\frac{1}{2}}} [-x_S y_S \sin g_T \cos I (4 + 3(x_S^2 + y_S^2)) - 5 \sin^2 I \times \\ & \times (1 - x_S^2 + 6y_S^2)) - 10(x_S y_S \sin g_T \cos I + x_S^2 \cos g_T) \cos^2 I (1 - \\ & - x_S^2 + 6y_S^2) - 10(1 - x_S^2 - y_S^2) x_S y_S \sin g_T (2 \cos^2 I - \sin^2 I) \times \end{aligned}$$

$$\begin{aligned} & \times \cos I] + \frac{\beta}{(1 - e_T^2)^2} x_S \cos I (1 - x_S^2 + 4y_S^2) + \frac{1}{(1 - e_T^2)^{\frac{3}{2}}} x_S \times \\ & \times \frac{2 - 2x_S^2 + 3y_S^2}{(1 - x_S^2 - y_S^2)^{\frac{1}{2}}} \end{aligned} \quad (39)$$

$$\begin{aligned} \frac{dg_T}{d\tau} &= \frac{1}{2} \frac{\beta}{(1 - e_T^2)^2} [4 + x_S^2 + 11y_S^2 - 5 \sin^2 I (1 - x_S^2 + 4y_S^2)] + \\ & + \frac{1}{(1 - x_S^2 - y_S^2)^{\frac{1}{2}} (1 - e_T^2)^{\frac{3}{2}}} \cos I (1 - x_S^2 + 4y_S^2) - \frac{5}{16} \alpha \beta \times \\ & \times \frac{1 + 4e_T^2}{(1 - e_T^2)^3 e_T} [(y_S \sin g_T \cos I + x_S \cos g_T) (4 + 3(x_S^2 + y_S^2)) - \\ & - 5 \sin^2 I (1 - x_S^2 + 6y_S^2)) - 10(1 - x_S^2 - y_S^2) \sin^2 I \cos I \times \\ & \times y_S \sin g_T] + \left(\frac{5}{16} \alpha \frac{e_T}{(1 - e_T^2)^{\frac{5}{2}}} \frac{1}{(1 - x_S^2 - y_S^2)^{\frac{1}{2}}} + \frac{5}{16} \alpha \beta \times \right. \\ & \times \frac{e_T}{(1 - e_T^2)^3} \cos I [-y_S \sin g_T (4 + 3(x_S^2 + y_S^2)) - 5 \sin^2 I (1 - \\ & - x_S^2 + 6y_S^2)) - 10(y_S \sin g_T \cos I + x_S \cos g_T) \cos I (1 - x_S^2 + \\ & + 6y_S^2) - 10(1 - x_S^2 - y_S^2) y_S \sin g_T (2 \cos^2 I - \sin^2 I)] \end{aligned} \quad (40)$$

$$\begin{aligned} \frac{de_T}{d\tau} &= \frac{5}{16} \frac{\alpha \beta}{(1 - e_T^2)^2} [(y_S \cos g_T \cos I - x_S \sin g_T) (4 + 3(x_S^2 + y_S^2)) - \\ & - 5 \sin^2 I (1 - x_S^2 + 6y_S^2)) - 10(1 - x_S^2 - y_S^2) y_S \sin^2 I \times \\ & \times \cos I \cos g_T] \end{aligned} \quad (41)$$

$$\begin{aligned} \frac{dI}{d\tau} &= - \frac{x_S \dot{x}_S + y_S \dot{y}_S}{(1 - x_S^2 - y_S^2)^{\frac{1}{2}}} \left(\frac{1}{\tan I (1 - x_S^2 - y_S^2)^{\frac{1}{2}}} + \frac{\beta}{\sin I (1 - e_T^2)^{\frac{1}{2}}} \right) - \\ & - \frac{e_T \dot{e}_T}{(1 - e_T^2)^{\frac{1}{2}}} \left(\frac{1}{\beta \sin I (1 - x_S^2 - y_S^2)^{\frac{1}{2}}} + \frac{1}{\tan I (1 - e_T^2)^{\frac{1}{2}}} \right) \end{aligned} \quad (42)$$

Acknowledgements

The author is grateful to Prof. Douglas Heggie for all the useful discussions on the context of this paper. The author also thanks Seppo Mikkola, who kindly provided the code for integrating hierarchical triple systems.

References

- Eggleton, P. and Kiseleva, L.: 1995, An empirical condition for stability of hierarchical triple systems, *Astroph. J.* **455**, 640-645.
- Ford, E.B., Kozinsky, B. and Rasio, F.A.: 2000, Secular evolution of hierarchical triple systems, *Astroph. J.* **535**, 385-401.
- Georgakarakos, N.: 2002, Eccentricity generation in hierarchical triple systems with coplanar and initially circular orbits, *MNRAS* **337**, 559-566.
- Kiseleva, L., Eggleton, P. and Mikkola, S.: 1998, Tidal friction in triple stars, *MNRAS* **300**, 292-302.
- Kozai, Y.: 1962, Secular perturbations of asteroids with high inclination and eccentricity, *Astron. J.* **67**, 591-598.
- Krymowski, Y. and Mazeh, T.: 1999, Studies of multiple stellar systems -II. Second-order averaged Hamiltonian to follow long-term orbital modulations of hierarchical triple systems, *MNRAS* **304**, 720-732.
- Marchal, C.: 1990, *The Three-Body Problem*, Elsevier Science Publishers, the Netherlands.
- Mikkola S.: 1997, Practical symplectic methods with time transformation for the few-body problem, *CeMDA* **67**, 145-165.
- Press, W., Teukolsky S., Vetterling W. and Flannery B.: 1996, *Numerical Recipes In Fortran 77*, 2nd ed., Cambridge Univ. Press, New York.

